Lipids in Health and Disease

RESEARCH

Open Access

Knockdown of RASD1 improves MASLD progression by inhibiting the PI3K/AKT/mTOR pathway

Guifang Zeng[1*†], Xialei Liu[1†], Zhouying Zheng[1†], Jiali Zhao[1], Wenfeng Zhuo[1], Zirui Bai[1], En Lin[1], Shanglin Cai[1], Chaonong Cai[1], Peiping Li[1*], Baojia Zou[1*] and Jian Li[1*]

Abstract

Background There is still no reliable therapeutic targets and effective pharmacotherapy for metabolic dysfunction-associated steatotic liver disease (MASLD). RASD1 is short for Ras-related dexamethasone-induced 1, a pivotal factor in various metabolism processes of Human. However, the role of RASD1 remains poorly illustrated in MASLD. Therefore, we designed a study to elucidate how RASD1 could impact on MASLD as well as the mechanisms involved.

Methods The expression level of RASD1 was validated in MASLD. Lipid metabolism and its underlying mechanism were investigated in hepatocytes and mice with either overexpression or knockdown of RASD1.

Results Hepatic RASD1 expression was upregulated in MASLD. Lipid deposition was significantly reduced in RASD1-knockdown hepatocytes and mice, accompanied by a marked downregulation of key genes in the signaling pathway of de novo lipogenesis. Conversely, RASD1 overexpression in hepatocytes had the opposite effect. Mechanistically, RASD1 regulated lipid metabolism in MASLD through the PI3K/AKT/mTOR signaling pathway.

Conclusions We discovered a novel role of RASD1 in MASLD by regulating lipogenesis via the PI3K/AKT/mTOR pathway, thereby identifying a potential treatment target for MASLD.

Keywords Ras-related dexamethasone-induced 1, MASLD, Lipid metabolism, PI3K/AKT/mTOR pathway

Introduction

Metabolic dysfunction-associated steatotic liver disease (MASLD) has become the most widespread liver disease and disorder globally, with the prevalence rates of 25.1–44.4% among adults and even 80% among individuals with diabetes and obesity [1–3]. The pathological processes of MASLD evolve from simple steatosis to steatohepatitis [3, 4], then develop to fibrosis and even worsen as end-staged diseases like cirrhosis and even hepatocellular carcinoma (HCC) in some cases [3, 4]. Moreover, occurrence of MASLD keeps on rising, outcome of which is the dramatic increase of patients with obesity and diabetes. Consequently, the burden imposed by MASLD-related HCC and liver transplantation is

†Guifang Zeng, Xialei Liu, and Zhouying Zheng contributed equally to this work.

*Correspondence:
Guifang Zeng
zenggf6@mail2.sysu.edu.cn
Peiping Li
lipp8@mail.sysu.edu.cn
Baojia Zou
zoubj6@mail.sysu.edu.cn
Jian Li
lijian5@mail.sysu.edu.cn
[1]Department of Hepatobiliary Surgery, The Fifth Affiliated Hospital of Sun Yat-sen University, Zhuhai, Guangdong 519000, People's Republic of China

escalating rapidly, presenting formidable challenges both economically and medically. However, due to its multifaceted nature involving numerous influencing factors, reliable therapeutic targets for MASLD remain elusive, with no officially approved specific drugs available for treatment. Therefore, it is urgent to identify crucial potential therapeutic targets during the early stage of simple steatosis to address this pressing issue.

The liver maintains lipid homeostasis by regulating fatty acid uptake, export, β-oxidation, and de novo lipogenesis (DNL) [5]. Hepatic steatosis is a condition with the excessive deposition of triglycerides (TG) in liver cells (hepatocytes) when this delicate balance is disrupted, which represents a hallmark pathological feature of MASLD [5, 6]. Numerous studies have increasingly demonstrated that increased DNL significantly contributes to hepatic lipid deposition [7–9]. The key enzymes involved in DNL are often regulated by sterol regulatory element-binding protein 1 (SREBP1) [10–12], an important transcriptional regulator of these enzymes [11], for example, Fatty acid synthase (FASN) and Acetyl-CoA carboxylase 1 (ACC1) [10–12]. Given the significance of DNL in hepatic steatosis and its potential therapeutic implications, further exploration and identification of novel feasible targets for modulating DNL will be beneficial.

RASD1(Dexras1) is short for Ras-related dexamethasone-induced 1, a member of the GTPases superfamily of Ras and highly upregulated by dexamethasone [13]. It is found to be expressed in various tissues across the human body, including the liver, heart, fat, brain, and lung, and shows significant homology between mice and humans [14]. Initial studies linked RASD1 with circadian rhythm regulation [15], which is closely related to diabetes and obesity [16–18], both of which are important pathogenic factors and extrahepatic features of MASLD [1]. Subsequent investigations have demonstrated that RASD1 is involved in insulin secretion, hepatic insulin resistance, and insulin-dependent antilipolysis [19–21]. Currently, it is generally accepted that insulin resistance and MASLD are closely interconnected [22–24]. Furthermore, studies have revealed that RASD1 mediates glucocorticoid-related adipocyte differentiation and diet-induced obesity [25–27]. Collectively, these results suggest that RASD1 may have important unknown impacts on MASLD. Therefore, we designed the study and investigated the role and mechanism of RASD1 in MASLD, hoping to discover its potential in diagnostic and therapeutic application for MASLD patients.

Methods

Human liver samples from our center

The human liver samples analysed in this study were collected from patients undergoing surgical treatment for benign abdominal diseases at our center (the Fifth Affiliated Hospital of Sun Yat-sen University) between March 2022 and March 2023. Criteria for diagnosis of MASLD was based on the latest Delphi consensus statement [1], and the hepatic steatosis diagnosis was made by two pathologists using liver biopsies. We collected liver samples from 15 patients diagnosed with MASLD as the MASLD group, and liver samples from 15 patients without liver steatosis, other chronic liver diseases, or malignant tumours were collected as the Normal group.

Cell culture and in vitro treatments

The human normal liver cells (hepatocytes LO2 cells) and the human hepatoma (HepG2 cells) were obtained as a gift from Cancer Center of Sun Yat-sen University (SYSUCC). They were kept and cultured in working medium prepared from complete Dulbecco's modified Eagle's medium with 10% fetal bovine serum as well as 1% penicillin–streptomycin (Gibco, New York, USA). To simulate hepatic steatosis in vitro, 1 mM free fatty acids (FFA) was used to incubate LO2 and HepG2 cells for 24 h [28, 29], and bovine serum albumin (BSA) (Sigma–Aldrich, New York, USA) without fatty acids served as the control.

To achieve stable overexpression or knockdown of RASD1 in LO2 and HepG2 cells, lentiviruses (Vigene Biosciences, Shandong, China) carrying vectors encoding RASD1 or short hairpin RNA (shRNA) targeting RASD1 were used for transfection (RASD1 or shRASD1 cell lines). Moreover, empty vectors or vectors encoding scramble shRNA served as their respective controls (Vector or Scramble cell lines). The shRNA sequences used were as follows: shRNA1, GGCCAAGAACTGCTATCG CATGGTTCAAGAGACCATGCGATAGCAGTTCTTG GCCTTTTTT; shRNA2, GGCGAGGTCTACCAGCTC GACATTTCAAGAGAATGTCGAGCTGGTAGACCTC GCCTTTTTT; and shRNA3, GGCTCAGGCAGCAGAT CCTCGACTTCAAGAGAGTCGAGGATCTGCTGCCT GAGCCTTTTTT. Following transfection for 48 h, stable cell lines were selected using a working medium supplemented with 2 ug/mL puromycin (MP Biomedicals, California, USA). Afterwards, the successfully established stable cell lines were also treated with FFA (at the concentration of 1 mM) for 24 h to investigate the specific role of RASD1 in lipid metabolism. Additionally, RASD1-overexpressing cell lines were pretreated with LY294002, rapamycin or MK2206 for one hour each. The concentrations of LY294002, MK2206, and rapamycin used to treat LO2 cells were 30 umol/L [30], 10 umol/L [31], and 20 nmol/L [28], respectively. For the HepG2 cells, the concentrations used were 20 umol/L [32], 1.7 umol/L [33], and 10 nmol/L [34]. All the inhibitors were purchased from MedChem Express (New Jersey, USA) and dissolved in DMSO (MP Biomedicals, California, USA).

Lipidomic analysis

LO2 stable cell lines treated with FFA (at the concentration of 1 mM) for 24 h were prepared for lipidomics analysis, ensuring a minimum of 1×10^6 cells per sample, and subsequently subjected to liquid extraction. The subsequent analysis was sent to and conducted by Wuhan Metware Biotechnology Co., Ltd (Wuhan, China). In brief, it includes ultra-performance liquid chromatography with related analysis and tandem mass spectrometry with related analysis.

Animal experiments

Twenty-two male C57BL/6J mice, at the age of 6 weeks, were purchased and transported to our center from Sperford Biotechnology Company (Beijing, China). We randomly divided 10 mice two groups 10 ($n=5$ for each): one group was fed a high-fat diet (HFD) (purchased as 60% fat, from Research Diets, New Jersey, USA) continuously for 12 weeks to induce hepatic steatosis (HFD group), whereas the other group was on a normal chow diet (NCD) (SPF-F02-001, Sperford Biotechnology Company, Beijing, China) (NCD group). We randomly assigned the remaining 12 mice into two groups ($n=6$ for each), all of which were on a HFD continuously for 12 weeks but also received tail vein injections every four weeks with adeno-associated virus serotype-8 (AAV8) (Vigene Biosciences, Shandong, China) at a dose of 5×10^{11} vg/mouse [35] during feeding. A total of three injections were administered, starting two weeks before HFD feeding. For AAV8-mediated RASD1 knockdown, the mice were injected with AAV8-CMV-shRASD1 (AAV-shRASD1/HFD group), and the corresponding control group (AAV-shNC/HFD group) was injected with AAV8-CMV-shNC. The sequences of the shRNAs targeting RASD1 were as follows: shRNA1, GCGACTCTGAACTGAGTATCCTTCAAGAGAGGATACTCAGTTCAGAGTCGCTTTTTT; shRNA2, GCTCAAACAGCAGATCCTAGATTCAAGAGATCTAGGATCTGCTGTTTGAGCTTTTTT; and shRNA3, GCGATGCCTTTGGCATCTTGGTTCAAGAGACCAAGATGCCAAAGGGCATCGCTTTTTT. The corresponding control shRNA had a scrambled nontargeted sequence: TTCTCCGAACGTGTCACGTTTCAAGAGAACGTGACACGTTCGGAGAATTTTT. The mice were weighed every 2 weeks from the beginning of HFD feeding. After 12 weeks, the mice were sacrificed via excess isoflurane anaesthesia after being fasted overnight. Blood and fresh tissues including livers, kidneys, and adipose tissues were quickly obtained for subsequent experiments.

Glucose and insulin tolerance test (GTT and ITT)

The GTT and ITT were performed in the tenth and eleventh weeks, respectively, according to our previously described methods [28]. Then we calculated the area under the curve (AUC) and area of the curve (AOC) for the GTT and ITT [36].

Biochemical analysis

Commercial assay kits were adopted to detect the expression levels of serum biomarkers including triglycerides (TG, A110-1-1), aspartate aminotransferase (AST, C010-2-1), glucose (GLU, A154-1-1), alanine aminotransferase (ALT, C009-2-1), and insulin (MM-0579M1). All kits were purchased from Jiangsu Meimian Industrial Co., Ltd (Jiangsu, China), except the ELISA kit (MM-0579M1, Nanjing Jiancheng Bioengineering Institute, China).

Real-time quantitative PCR (qPCR)

A Total RNA Isolation Kit was used, for preparation of the total RNA extracted from fresh liver tissues (human and animal) as well as cultured cells using, and then a Reverse Transcription Kit for qPCR was used for synthesis of the cDNA used for following qPCR detectioni. Subsequently, qPCR was performed according to the manufacturer's instruction, using SYBR qPCR Master Mix kit on a CFX Connect real-time system (Bio-Rad, California, USA). The above three kits were obtained from Vazyme (Nanjing, China). The primer sequences were synthesized by Invitrogen and are available upon request. Gene expression levels were determined by Ct values, normalized to β-actin ($2^{-\triangle\triangle Ct}$ method).

Western blotting (WB)

In brief, total protein samples were extracted from tissues and cells of human and mice origin. They were prepared, loaded and then separated in SDS-PAGE gel, before transferring to PVDF membranes. Following a blocking step with 5% skim milk, membranes were incubated with primary antibody specific to the protein target (overnight, 4 °C). Afterwards, the secondary antibody were applied for incubation (1 h, room temperature). Finally, the blots were acquired using ECL reagent in the automatic chemiluminescence image analysis system (Tanon, Shanghai, China) and they were analysed using the ImageJ software (NIH, Maryland, USA).

The antibodies applied in the WB experiments were as follows: RASD1 (A05991-1, BOSTER, Wuhan, China); β-actin (CPA1009) and SREBP1 (CPA7189) from Cohesion Biosciences (Suzhou, China); ACC1 (4190), FASN (3180), mTOR (2792), p-mTOR (2791), AKT (9272), p-AKT (4060), PI3K p85 (4292), p-PI3K p85 (4228), PI3K p110α (4249), and horseradish peroxidase -linked goat anti-rabbit IgG (7074) (Cell Signaling Technology/CST, Massachusetts, USA); and S6K (A2190), p-S6K (AP1389), IR (A19067), p-IR (AP1352), IRS1 (A0245), and p-IRS1 (AP0552) from ABclonal Biotechnology Co., Ltd (Wuhan, China).

Chemical staining assays

Paraffin-embedded samples (liver tissues) were prepared as 4–5 μm sections. They were used for hematoxylin-eosin(HE) staining and immunohistochemical (IHC) staining using an HE staining kit (G1005, Servicebio, Wuhan, China) and an IHC staining kit (SA1028, BOSTER, Wuhan, China), respectively. For immunofluorescent (IF) staining, the IHC experimental procedure was followed until the primary antibody (RASD1, A05991-1, BOSTER, Wuhan, China) was incubated. Afterwards, the sections were incubated with fluorescent secondary antibodies (ab150077, Abcam, Massachusetts, USA) for 1 h and then stained with DAPI (Solarbio, Beijing, China) for 10 min. However, cultured cells were prepared and fixed for IF staining using the 4% paraformaldehyde for 15 min (Biosharp, Hefei, China) and, then permeated using the 0.1% Triton X-100 (Macklin, Shanghai, China) for another 5 min. The subsequent experiments were performed in the same way as those described for the liver sections. For oil red O (ORO) staining, cultured cells and frozen liver Sects. (8–10 μm) were stained with an ORO Staining Kit (Beyotime, Shanghai, China) [28]. All the representative images were acquired using an optical microscope or a confocal microscope (Zeiss, Oberkochen, Germany), and analysed using ImageJ software [28].

Statistical analysis

For statistical analysis, GraphPad Prism (version 9.0, California, USA) was adopted. The continuous variables are shown as the means ± SDs. Student's t test was used as well as one-way ANOVA were used for two or more groups and factors involved. Categorical variables are shown and presented as numbers (%), analyzed by the χ^2 test in SPSS 21.0 (IBM, New York, USA). For each test, $P<0.05$ was considered as statistically significant.

Table 1 General clinical characteristics of the 30 patients evaluated

Characteristics	Normal group	MASLD group	*P*
	n = 15	*n* = 15	
Sex			0.456
Male	10(66.7%)	8(53.3%)	
Female	5(33.3%)	7(46.7%)	
Age, years	47.67 ± 10.94	48.73 ± 11.80	0.799
BMI, kg/m*2*	25.00 ± 2.22	27.37 ± 5.49	0.387
Plasma ALT, U/L	42.79 ± 46.96	32.23 ± 15.51	0.416
Plasma AST, U/L	32.28 ± 23.97	41.95 ± 71.37	0.623
Plasma ALP, U/L	87.67 ± 54.12	72.93 ± 25.50	0.348
Plasma GGT, U/L	124.51 ± 153.81	105.07 ± 151.38	0.730
Serum TG, mmol/L	1.39 ± 0.55	2.63 ± 2.03	0.037*
Serum TCHO, mmol/L	3.95 ± 0.71	4.85 ± 1.15	0.016*
Serum HDL-C, mmol/L	1.16 ± 0.34	1.19 ± 0.32	0.797
Serum LDL-C, mmol/L	2.45 ± 0.76	2.31 ± 0.93	0.642
Serum GLU, mmol/L	5.25 ± 0.53	7.09 ± 2.76	0.023*
Type 2 diabetes	0(0%)	9(60%)	0.001**
Yes	15(100%)	6(40%)	
No			

*$P<0.05$, **$P<0.01$. Continuous variables presented in the table are in the form of means ± SDs, whereas categorical variables presented in the table are in the form of numbers (%)

Results

Hepatic RASD1 expression significantly increased in MASLD patients

We initially assessed the expression level of RASD1 in human hepatic tissues, which were derived from either the normal population or MASLD patients. The clinical characteristics are summarized and shown in Table 1. Because the included MASLD patients analyzed in this study were all in the early stage of simple hepatic steatosis and a few belonged to the 'lean MASLD' category [37], some of the analyzed data was less significant when comparing the two groups, including the body mass index (BMI), plasma levels of the liver function tests (ALP, ALT, GGT, AST), as well as the serum levels of lipoproteins (high-density/HDL-C and low-density/LDL-C). However, patients with MASLD presented significantly greater levels of fasting serum GLU, total cholesterol (TCHO), serum TG, and most patients in the MASLD group also had type 2 diabetes, which conformed to the Delphi consensus statement [1].

Hepatic RASD1 expression were significantly increased in the MASLD group of patients on both the mRNA levels and the protein levels, while the HE staining results revealed numerous vacuolar lipid droplets (Fig. 1A-C). Consistently, IHC and IF staining revealed increased expression of RASD1, with RASD1 protein primarily expressed in the cell nucleus and cytoplasm (Fig. 1C, D).

RASD1 expression was elevated in FFA-treated hepatocytes

We subsequently investigated the potential role of RASD1 in FFA-treated hepatocytes. ORO staining revealed significant increases in intracellular lipid deposition in both LO2 and HepG2 cell lines treated with FFA (Fig. 2A). Moreover, the intracellular levels of TG were significantly elevated (Fig. 2B), accompanied by upregulation of the ACC1, FASN, and SREBP1 proteins (Fig. 2C). These results confirmed that the hepatic steatosis model in vitro was established successfully. Consistent with our findings from human liver tissues, RASD1 were significantly increased in FFA-treated hepatocytes at both the mRNA levels and the protein levels (Fig. 2C-D), and stronger fluorescence signals were detected in the nucleus and cytoplasm (Fig. 2E-F). In summary, these data demonstrated the significant upregulation of RASD1 during the process of hepatic steatosis in vitro.

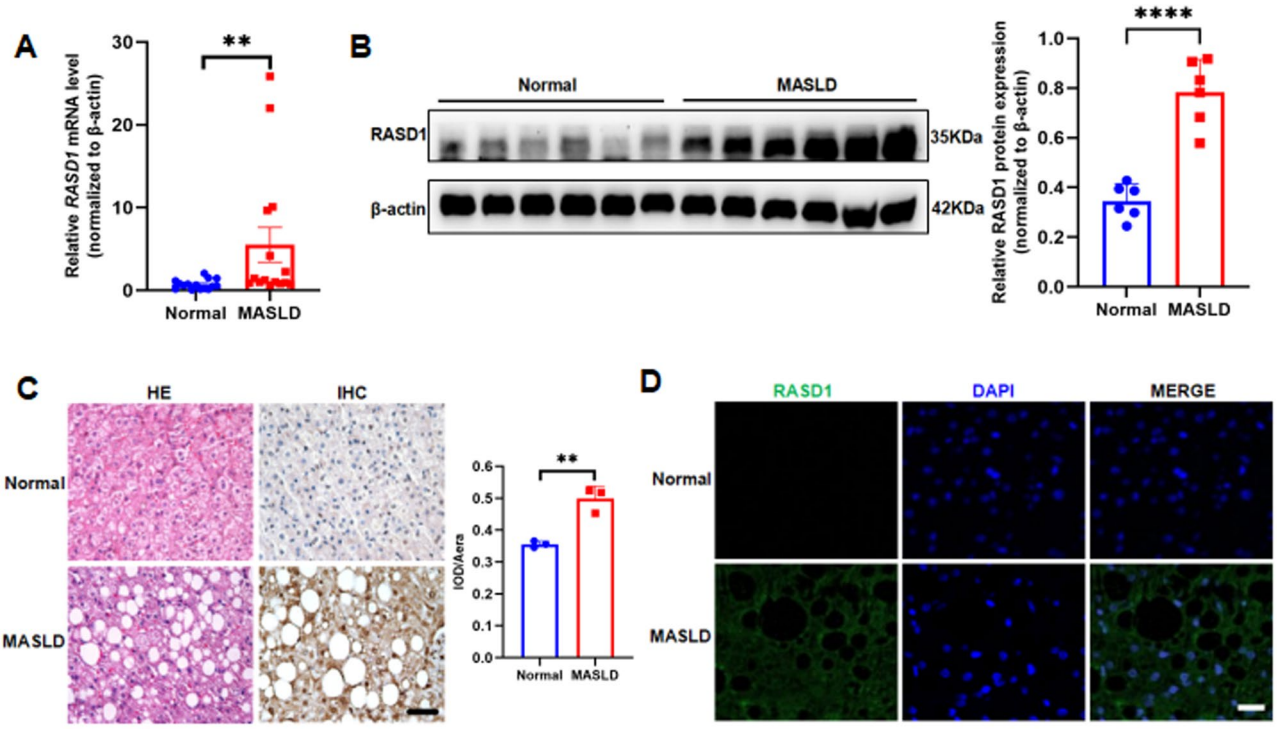

Fig. 1 Hepatic RASD1 was upregulated in patients with MASLD. (**A**) qPCR analysis showing the RASD1 mRNA expression levels in liver tissues from both groups ($n=15$ each). (**B**) WB analysis of RASD1 protein levels and the corresponding quantitative analysis of liver tissues from the Normal and MASLD groups ($n=6$). (**C**) Representative HE and IHC staining of liver tissues from the Normal and MASLD groups (scale bar, 50 μm), on the right of which the IHC staining data is quantified and shown ($n=3$). (**D**) Representative IF staining of liver tissues from the Normal and MAFLD groups (scale bar: 20 μm). $^{**}P<0.01$, $^{****}P<0.0001$, comparing to those data of the Normal group. All data presented in the figure are means ± SDs

Overexpression of RASD1 enhanced lipid deposition in FFA-treated hepatocytes

To elucidate the specific role of RASD1 in MASLD, we used RASD1-overexpressing lentiviruses to infect LO2 and HepG2 cells (Fig. 3A, B). The stable cell lines were subsequently exposed to 1 mM FFA for the duration of 24 h. Compared to the negative control cell lines (Vector), the RASD1 cell lines presented significant increases in lipid deposition and intracellular TG levels (Fig. 3C-D). Furthermore, lipidomic analysis revealed increased synthesis of TG in LO2 RASD1 cell lines (Fig. 3E). Moreover, the qPCR results indicated that *RASD1* had the greatest effect on the upregulation of genes related to DNL but had little impact on genes involved in fatty acid esterification (except *diacylglycerol o-acyltransferase 2,DGAT2*), β-oxidation (except *hydroxysteroid 17-beta dehydrogenase 4,HSD17B4*), uptake (except *fatty acid binding protein 2,FABP2*) and export (except *apolipoprotein B*, i.e. *APOB* and *microsomal triglyceride transfer protein*, i.e. *MTTP*) in LO2 RASD1 cell lines (Fig. 3F). Additionally, the protein levels of DNL-related genes were upregulated in both LO2 and HepG2 RASD1 cell lines (Fig. 3G). In summary, RASD1 overexpression enhanced the deposition of lipid in the FFA-treated hepatocytes.

RASD1 knockdown inhibited lipid deposition in FFA-treated hepatocytes

To further validate the aforementioned role of RASD1 on hepatic lipid metabolism, we established stable RASD1 knockdown in LO2 and HepG2 cells (Fig. 4A, B), which were subsequently treated by 1 mM FFA for 24 h. In contrast to RASD1 overexpression, RASD1 knockdown obviously reduced lipid accumulation and intracellular TG in shRASD1 cell lines compared with those in Scramble cell lines (Fig. 4C-D). Furthermore, lipidomic analysis further confirmed that RASD1 knockdown markedly suppressed TG synthesis in LO2 shRASD1 cell line (Fig. 4E). Additionally, the qPCR results indicated that *RASD1* knockdown had the most significant effect on downregulating genes in DNL and fatty acid esterification (except *DGAT2*) but had minimal influence on genes in β-oxidation (except *HSD17B4*), uptake and export (except *APOB*) of fatty acid in LO2 shRASD1 cell lines (Fig. 4G). Moreover, DNL genes were significantly downregulated in both shRASD1 cell lines at protein levels (Fig. 4H). Therefore, our findings suggested that RASD1 knockdown inhibited lipid deposition in FFA-treated hepatocytes.

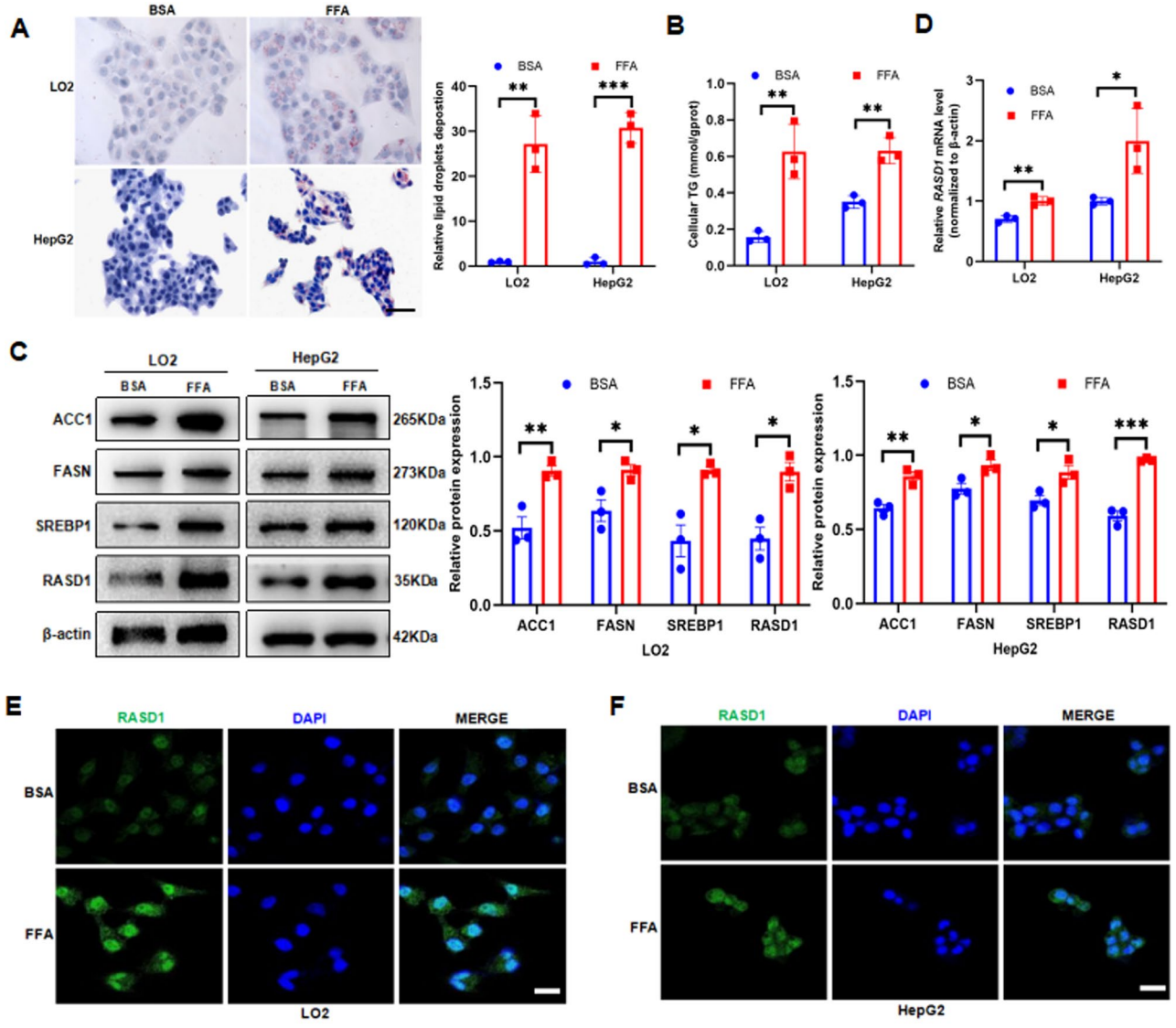

Fig. 2 RASD1 expression was elevated in FFA-treated hepatocytes. (**A**) Representative ORO staining of hepatocytes that were treated with BSA or FFA and the corresponding quantitative analysis are presented on the right (scale bar: 50 μm). (**B**) Cellular TG content of hepatocytes that were treated with BSA or FFA. (**C**) WB determination and the quantification of the *RASD1* protein in hepatocytes, with or without FFA or BSA treatment. (**D**)*RASD1* mRNA levels were shown by qPCR analysis results, of hepatocytes treated with BSA or FFA. **(E**, **F)** Representative IF staining images of hepatocytes treated by either BSA or FFA (the scale bar shown as 20 μm). $n = 3$ in all groups. $^{*}P < 0.05$, $^{**}P < 0.01$, $^{***}P < 0.001$, as are compared to BSA treatment. All data presented in this figure here are means ± SDs

RASD1 modulated lipid metabolism in hepatocytes by PI3K/AKT/mTOR signaling pathway

RASD1 belongs to Ras superfamily and possesses a Ras-like domain [13], and PI3K/AKT/mTOR is an important and common signaling pathway regulating lipid metabolism, activated by Ras [38–40] and closely associated with MASLD [41–48]. Therefore, we investigated whether RASD1 modulates cellular lipid metabolism via the Therefore, we initially detected the protein levels of PI3K, AKT, mTOR, and the downstream effector of mTOR, i.e. p70 S6 Kinase (S6K), as well as the phosphorylation status of the protein targets: mTOR at S2448 (p-mTOR), and at S6K at T389 (p-S6K), AKT at Ser473 (p-AKT), PI3K at p85 (p-PI3K), in stable cell lines. Compared to the control (vector), RASD1 overexpression led to increased phosphorylation levels of the detected proteins of PI3K, AKT, mTOR and S6K (Fig. 5A). In contrast, RASD1 knockdown resulted in opposite results compared with those of the Scramble cell line (Fig. 5B). Meanwhile, we treated the Scramble and shRASD1 cell lines with cycloheximide (CHX, 50 μg/mL) to examine the effect of RASD1 on PI3K protein degradation, for 0, 6 and 12 h [49]. The results showed that RASD1 knockdown accelerated PI3K protein degradation (Supplementary Fig. 1).

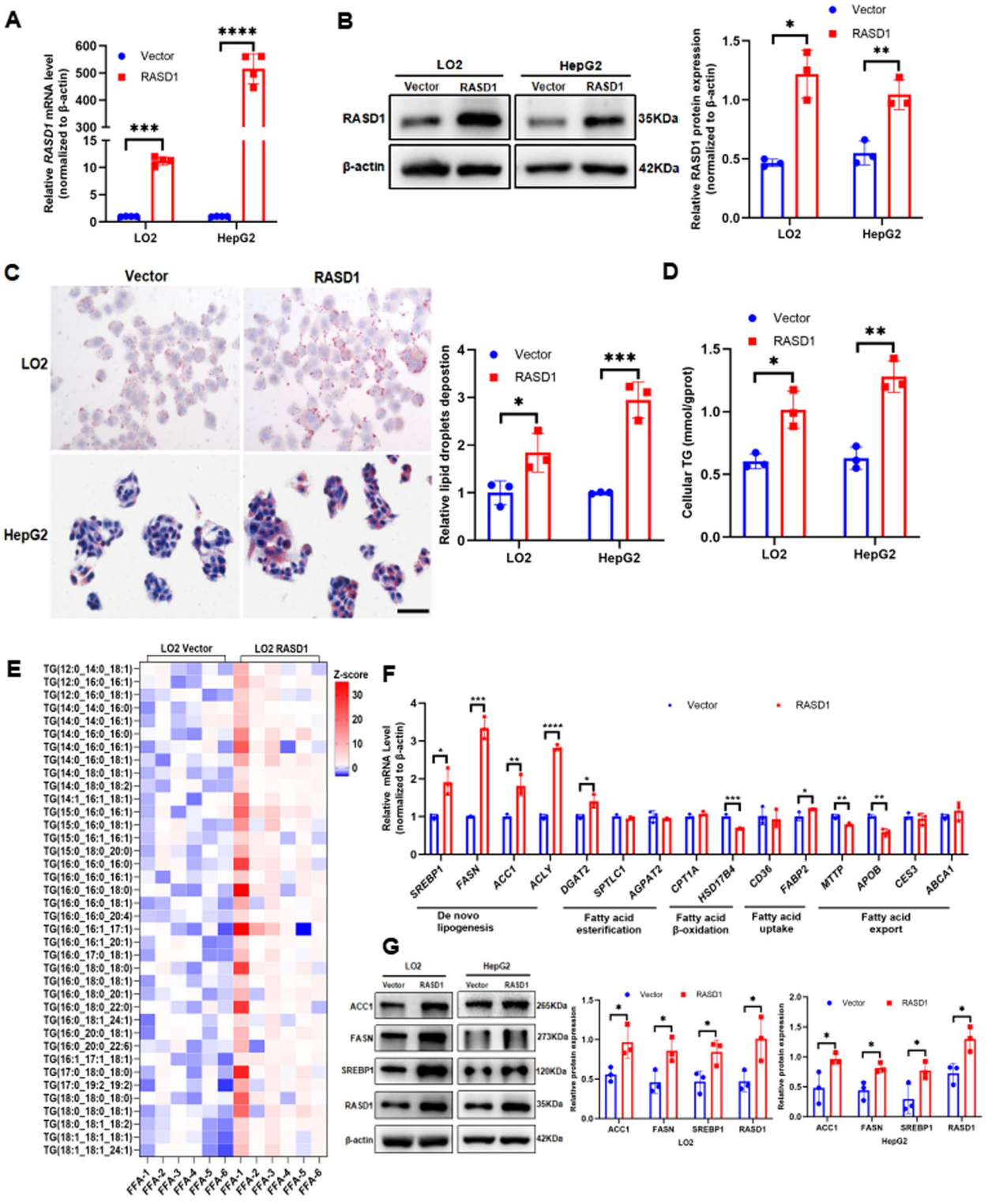

Fig. 3 Overexpression of RASD1 promoted lipid deposition in FFA-treated hepatocytes. **(A, B)** The successful overexpression of RASD1 was confirmed by qPCR and WB ($n=3$–4). The protein levels of RASD1 is quantified and shown on the right. (**C**) Representative ORO staining of Vector and RASD1 cell lines (scale bar: 50 μm). The corresponding quantitative analysis is presented on the right ($n=3$). (**D**) Cellular TG contents of the Vector and RASD1 cell lines ($n=3$). (**E**) Lipidomic analysis further demonstrated that TG synthesis was increased in the LO2 RASD1 cell line ($n=6$). (**F**) Gene expression in lipid metabolism of the LO2 RASD1 cell line was measured and determined by qPCR. (**G**) WB determination of the protein levels was quantified in the Vector and RASD1 cell lines ($n=3$). As are compared to Vector, $^{*}P<0.05$, $^{**}P<0.01$, $^{***}P<0.001$, $^{****}P<0.0001$. All data presented in the figure are means ± SDs

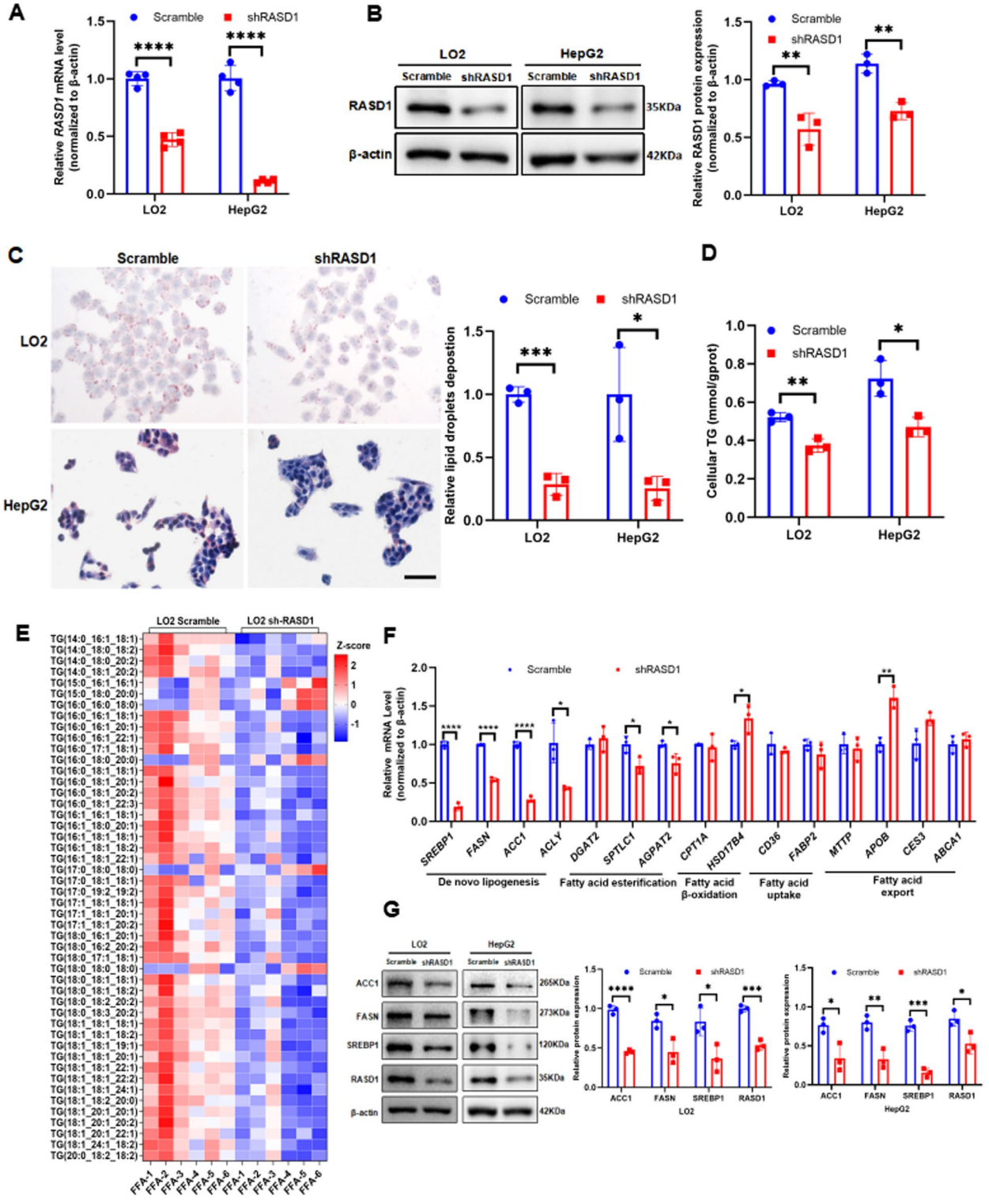

Fig. 4 RASD1 knockdown inhibited lipid deposition in FFA-treated hepatocytes. **(A**, **B)** The successful knockdown of RASD1 was confirmed by qPCR and WB ($n=3$–4). The protein levels of RASD1 are quantified and shown on the right. (**C**) Representative ORO staining of the Scramble and shRASD1 cell lines with the corresponding quantification ($n=3$, the scale bar shown as 50 μm). (**D**) Cellular TG contents derived from the Scramble and shRASD1 cell lines ($n=3$). (**E**) Lipidomic analysis further demonstrated that TG synthesis was increased in the LO2 shRASD1 cell line ($n=6$). (**F**) Gene expression of lipid metabolism in the LO2 shRASD1 cell line was measured by qPCR. (**G**) The quantification of WB detection in the Scramble and shRASD1 cell lines($n=3$). As comparing to Scramble as control, $^{*}P<0.05$, $^{**}P<0.01$, $^{***}P<0.001$, $^{****}P<0.0001$. Unless otherwise noted, all data presented in the figure are means ± SDs

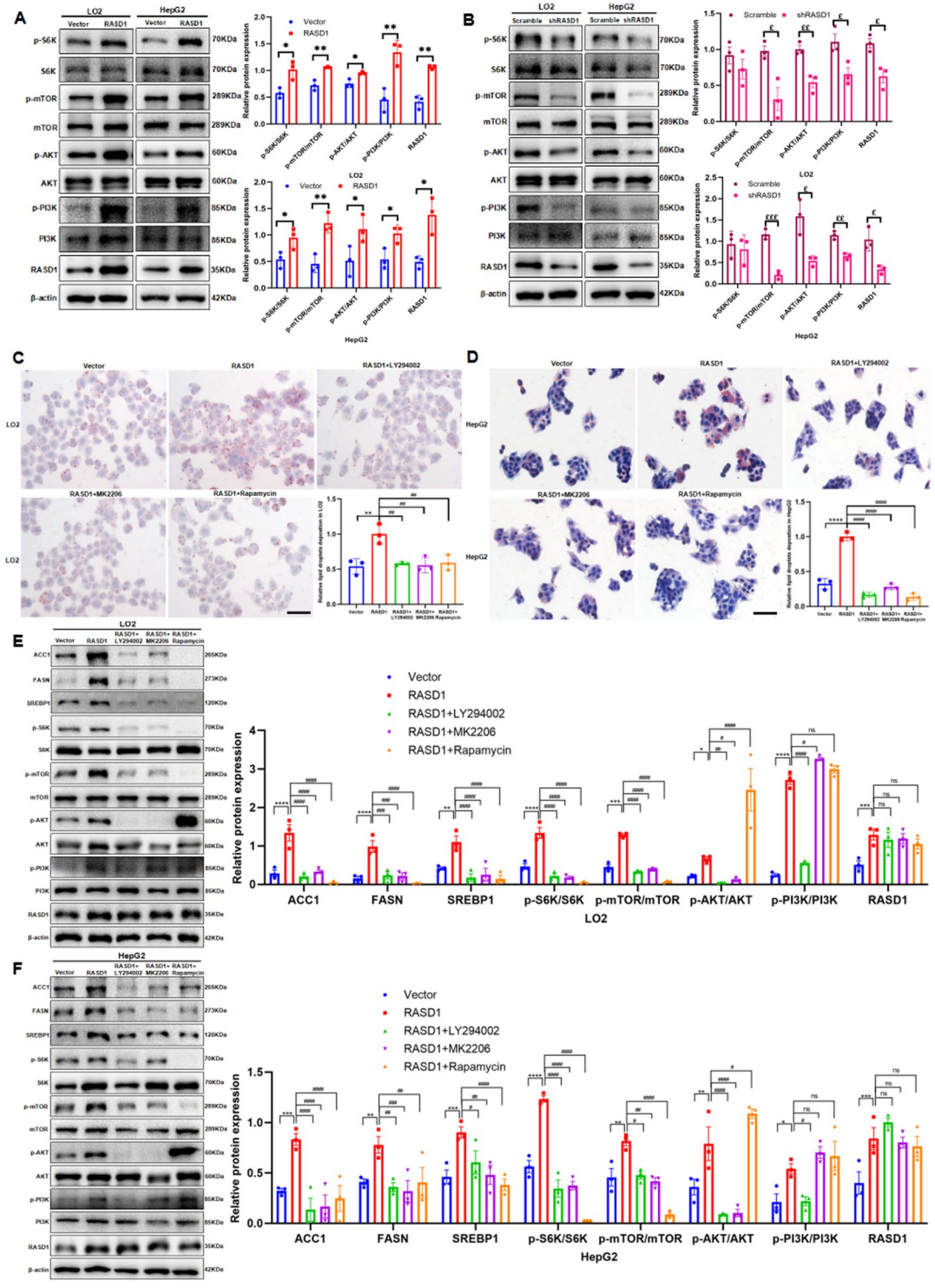

Fig. 5 RASD1 modulated cellular lipid metabolism via PI3K/AKT/mTOR pathway. **(A**,**B)** WB and the corresponding quantitative analysis of the expression of the pathway in stable cell lines ($n=3$). **(C**, **D)** Representative ORO staining of the stable cell lines treated with 1 mM FFA with or without inhibitors for 24 h (scale bar shown as 50 μm) and the corresponding quantification ($n=3$). (**E-F**) WB analysis and its quantification results, in the stable cell lines treated in1 mM FFA, with or without inhibitors for 24 h ($n=3$). As compared to Vector, $^{*}P<0.05$, $^{**}P<0.01$, $^{***}P<0.001$, $^{****}P<0.0001$ vs. Vector; As compared to Scramble, $^{£}P<0.05$, $^{££}P<0.01$, $^{£££}P<0.001$; $^{\#}P<0.05$, $^{\#\#}P<0.01$, $^{\#\#\#}P<0.001$, $^{\#\#\#\#}P<0.0001$, as compared to RASD1. Unless otherwise noted, all the data presented in the figure are means ± SDs

To further confirm that RASD1 modulates cellular lipid metabolism in hepatocytes by PI3K/AKT/mTOR signaling pathway, we employed specific inhibitors, including a PI3K inhibitor (LY294002), an AKT inhibitor (MK2206), and an mTOR inhibitor (rapamycin), to suppress the phosphorylation of the proteins of PI3K, AKT, and mTOR, respectively, in FFA-treated RASD1 cell lines. Subsequent ORO staining revealed that lipid accumulation was no longer increased in the presence of these inhibitors in RASD1 cell lines (Fig. 5C-D). Moreover, the downregulation of ACC1, FASN, and SREBP1 expression was observed thereafter (Fig. 5E-F). Meanwhile, the expression levels of phosphorylated proteins of AKT, mTOR, and S6K was inhibited following PI3K inhibition. The results showed that RASD1 activated AKT and mTOR by PI3K (Fig. 5E-F). Collectively, these findings provide compelling evidence supporting that RASD1 regulates hepatic lipid metabolism by activating PI3K/AKT/mTOR pathway.

RASD1 knockdown improved MASLD development in HFD-fed mice

Next, we confirmed our findings of RASD1 in regulation of hepatic lipid metabolism in vivo. We built an MASLD mouse model by HFD feeding and used AAV8 to knock down RASD1 in mouse livers. The experimental design is depicted schematically in Fig. 6A. First, qPCR, WB, and IHC experiments revealed significant upregulation of RASD1 in the livers the mice with HFD (Fig. 6B-D). Moreover, AAV8-CMV-shRASD1 effectively knocked down RASD1 in the livers but not in the adipose tissues or kidneys of AAV-shRASD1/HFD group (Fig. 6B-D, Supplementary Fig. 2). Encouragingly, livers from both HFD and AAV-shNC/HFD group appeared enlarged with light yellow colouration and dull edges—features of fatty liver, whereas livers from AAV-shRASD1/HFD group appeared smaller with reddish colouration and sharp edges, similar to those of the NCD group (Fig. 6D). HE and ORO staining further confirmed that RASD1 knockdown notably reduced the lipid droplet numbers in the liver, as compared to those in HFD and AAV-shNC/HFD group (Fig. 6D). In addition, compared with NCD group, HFD-induced obese mice presented a noticeable increase in body weight (Fig. 6E), along with significant increases in the AUC and AOC in the GTT and an increase in the AUC but a decrease in the AOC in the ITT, (Fig. 6F-K), all of which indicate the development of insulin resistance. Conversely, AAV-shRASD1/HFD group displayed reduced body weight gain (Fig. 6E) and AUC in the GTT and ITT, and a decreased AOC in the GTT but an insignificant increased AOC in the ITT (Fig. 6F-K), suggesting that RASD1 knockdown may ameliorate HFD-induced obesity and insulin resistance. Furthermore, biochemical analysis revealed significantly increase of ALT, AST, GLU, insulin and TG levels in the serum as well as greater TG contents in liver tissues from the HFD-fed group of mice, whereas RASD1 knockdown reversed this trend, except for liver function (Fig. 6L-Q). Together, our results suggested that RASD1 knockdown improved MASLD progression, including hepatic steatosis development, obesity and insulin resistance.

RASD1 knockdown inhibited DNL-related genes and the PI3K/AKT/mTOR pathway but restored the insulin signalling in HFD-fed mice

Then we sought to verify the potential mechanism of RASD1 in lipid metabolism in vivo. We evaluated the expression levels of key genes involved in DNL, the PI3K/AKT/mTOR pathway and the insulin signalling in the mice liver tissues from four groups. Our results revealed significant upregulation of the ACC1, FASN, and SREBP1 proteins in HFD-fed mice, accompanied by increased phosphorylation of PI3K, AKT, mTOR, and S6K, but decreased phosphorylation levels of the insulin receptor (p-IR) as well as that of the insulin receptor substrate 1 (p-IRS1) (Fig. 7A, B). However, RASD1 knockdown reversed this trend (Fig. 7C, D). Consistent with our previous in vitro results, these data provide further evidence that RASD1 knockdown inhibited hepatic DNL-related genes and the PI3K/AKT/mTOR pathway.

Discussion

Exploring the important regulators of the lipid metabolism in liver is expected to aid in treating or preventing the development of MASLD [6]. Before this study, the specific role of RASD1 in MASLD remained unknown. Previous studies have investigated the metabolic roles of RASD1 on secretion of insulin and its ability to mediated antilipolysis [19–21], glucocorticoid-mediated adipocyte differentiation and diet-induced obesity [25–27], suggesting a prominent adipogenic role for RASD1. However, here we show that RASD1 also plays a lipogenic role in MASLD independent of glucocorticoids. Although both processes contribute to fat accumulation, they are fundamentally distinct. The former promotes adipocyte differentiation, leading to increased adipose tissue and subsequent obesity, whereas the latter represents abnormal lipid accumulation in the liver, where fat is not typically stored under normal conditions—a manifestation of disrupted lipid metabolism disorder. However, these two processes are closely intertwined in the pathogenesis of MASLD because impaired insulin signalling or insulin resistance in adipocytes results in dysregulated lipolysis and exacerbates lipid influx into the liver beyond normal levels [23]. Furthermore, elevated insulin levels will promote hepatic DNL in patients with MASLD [22]. In turn, disturbances in lipid metabolism can directly impact insulin signalling pathways, thereby impairing insulin

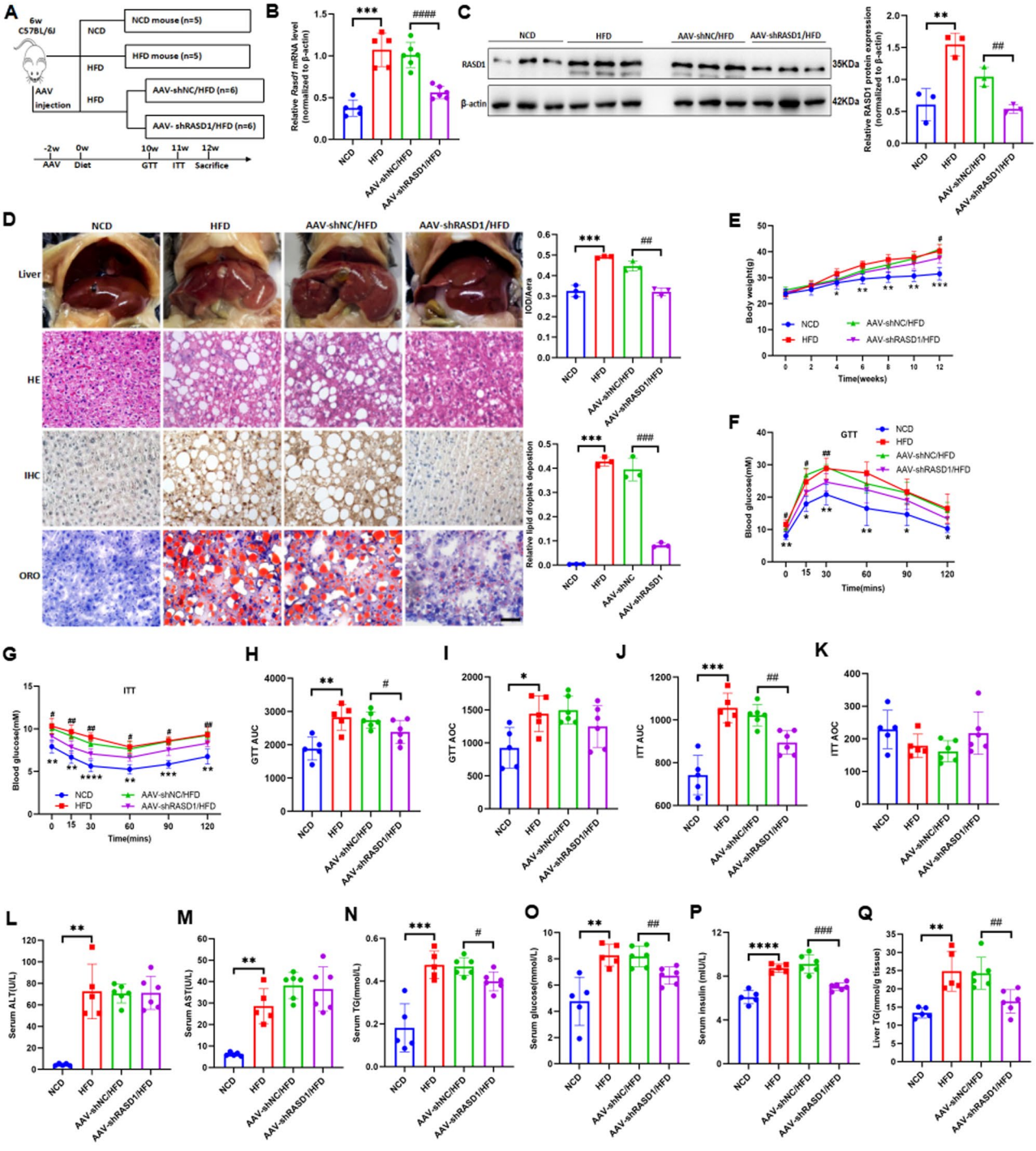

Fig. 6 RASD1 knockdown improved MASLD development in vivo. (**A**) Schematic diagram of the animal study. (**B**) Hepatic *Rasd1* mRNA levels in mice from four groups ($n = 5–6$). (**C**) Hepatic RASD1 protein levels and the corresponding quantitative analysis of mice from four groups ($n = 3$). (**D**) Representative images showing the gross look of the liver as well as staining of HE, IHC and ORO under microscope (scale bar: 50 μm) of mice from four groups. The quantitative analysis results of IHC and ORO staining are shown on the right ($n = 3$). (**E**) Body weights of the mice from four groups ($n = 5$). (**F**, **G**) results of the GTT and ITT detected in different time in the mice assigned to each group ($n = 5–6$). **(H-K)** AUC and AOC for the GTT and ITT results ($n = 5–6$). (**L-P**) Serum levels of liver function assays and insulin in the mice from four groups ($n = 5–6$). (**Q**) TG levels in the mice liver tissues from four groups ($n = 5–6$). With the NCD group as control comparison, $^{*}P < 0.05$, $^{**}P < 0.01$, $^{***}P < 0.001$, $^{****}P < 0.0001$; With the AAV-shNC/HFD group as control comparison, $^{\#}P < 0.05$, $^{\#\#}P < 0.01$, $^{\#\#\#\#}P < 0.0001$, which are compared to the group. All data presented in the figure are means ± SDs

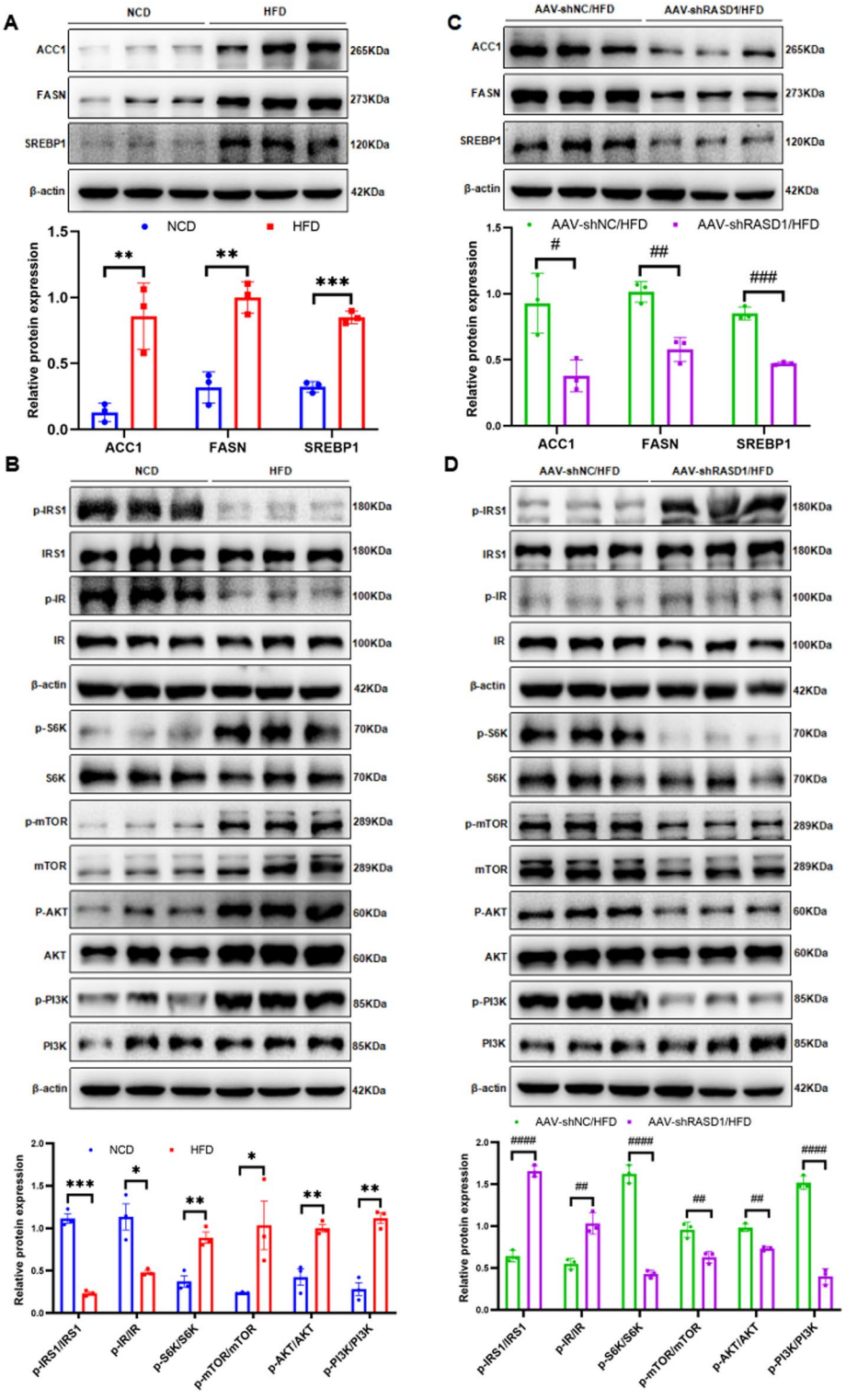

Fig. 7 RASD1 knockdown inhibited hepatic DNL-related genes and PI3K/AKT/mTOR signaling but restored the insulin signaling in the HFD-fed mice model. **(A-D)** WB analysis and corresponding quantification detecting DNL-related genes, PI3K/AKT/mTOR signaling and the insulin signalling in the liver tissues from the NCD, HFD, AAV-shNC/HFD and AAV-shRASD1/HFD groups of mice ($n=3$). As are compared to the NCD group, $^{*}P<0.05$, $^{**}P<0.01$, $^{***}P<0.001$, $^{****}P<0.0001$; $^{\#}P<0.05$, $^{\#\#}P<0.01$, $^{\#\#\#}P<0.0001$, which are compared to the AAV-shNC/HFD group. All data shown in the figure are presented as means ± SDs

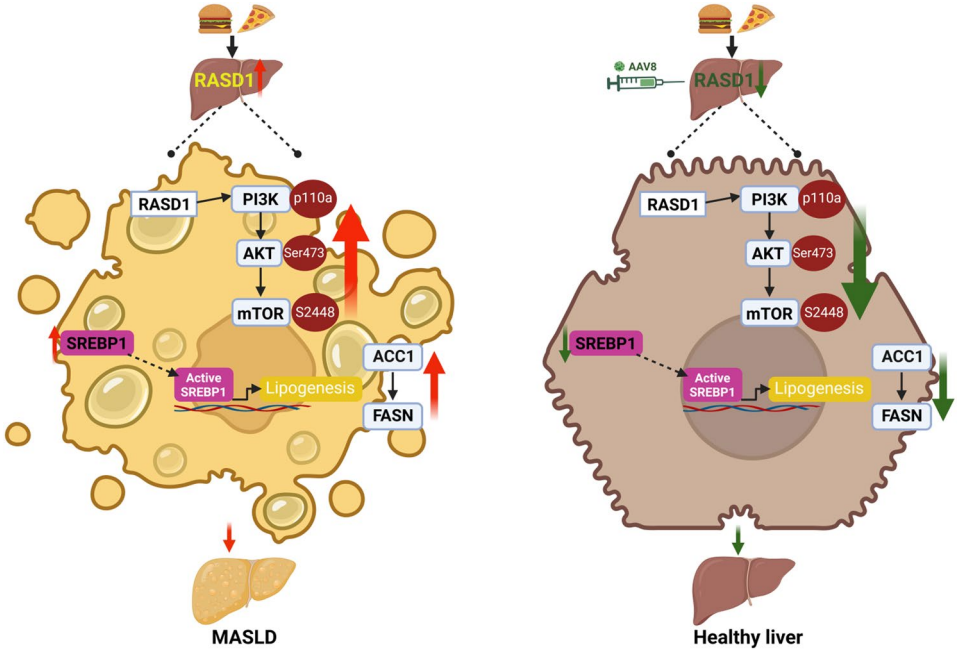

Fig. 8 Graphical abstract of this study. Hepatic RASD1 expression is upregulated in MASLD induced by HFD. When hepatic RASD1 is knocked down using AAV, the PI3K/AKT/mTOR signaling is thus inhibited, which prevents MASLD by suppressing DNL-related genes including SREBP1, ACC1, and FASN [Image created using bioRender]

secretion and eventually leading to insulin resistance and glucose metabolism disorders [24].

In this study, RASD1 was upregulated during hepatic steatosis. Importantly, RASD1 knockdown reduced the TG contents. It suggests that RASD1 is a pivotal factor in TG metabolism for liver. Additionally, RASD1 knockdown reduced HFD-induced weight gain, although the effect was not as pronounced as that reported by Cha et al. [25]. This discrepancy could be attributed to the use of systemic RASD1 knockout mice, which significantly reduced adipose tissue mass compared with our approach using AAV8-mediated knockdown, which specifically targeted the liver while having minimal impact on adipose tissue in mice. Unfortunately, to ensure the knockdown effect of AAV8 in our study, we administered multiple high-dose AAV8 injections to the mice, which may be toxic to the livers of the mice [50, 51]. And this may explain why the serum liver function tests of the AAV-shRASD1/HFD group did not decrease. Furthermore, consistent with previous research suggesting that Coreopsis tinctoria ameliorates HFD-induced hyperinsulinaemia by downregulating RASD1 [20], current study further indicate that RASD1 knockdown improved insulin resistance in HFD-fed mice. Considering that RASD1 is an insulin secretion gene [20], it is reasonable that a HFD leads to the upregulation of RASD1 and excessive insulin secretion, ultimately resulting in hyperinsulinaemia accompanied by insulin resistance, rather than insufficient insulin secretion, causing hyperglycaemia. Therefore, RASD1 knockdown is promising for alleviating these phenomena by enhancing insulin sensitivity through the restoration of impaired insulin signalling.

Mechanistically, consistent with previous research, this study verified that RASD1 promotes hepatic steatosis by activating the PI3K/AKT/mTOR pathway [38–43]; therefore, inhibit it can improve MASLD [44–48]. Moreover, mTORC1 can promote the SREBP1 activation with or without the involvement of S6K1 pathway and ultimately stimulating the hepatic DNL [52–55]. However, further investigation is needed to determine whether RASD1 activates SREBP1 via an S6K-dependent or S6K-independent pathway in our study. Notably, the PI3K/AKT signalling is an important regulation route for maintaining insulin and glucose homeostasis, which is activated when stimulated with insulin [56, 57]. However, paradoxically, the observed reduction in AKT phosphorylation contradicts the increase in insulin sensitivity in AAV-shRASD1/HFD group, although p-IR and p-IRS1 were indeed upregulated. This may be because RASD1 may directly regulate the insulin signaling pathway or because under conditions of chronic hyperinsulinaemia induced by a HFD, AKT is continuously phosphorylated, while p-IR and p-IRS1 are depleted, which ultimately promotes lipid lipogenesis [22]. Moreover, it should be mentioned that the role of AKT in MASLD is still controversial, as different studies have revealed contradictory results. In addition to the findings of numerous studies, which are consistent with our results [41–48], other studies pointed out that AKT activation inhibits lipid synthesis [58, 59].

Although there is no consensus on this matter, it does suggest that AKT is a crucial participant in MASLD.

Strengths and limitations

This study shows it here that RASD1 was significantly increased in MASLD, which suggested that RASD1 may be used to predict MASLD. RASD1 knockdown can significantly inhibit hepatic DNL-related genes, thereby alleviating hepatic steatosis, obesity, and insulin resistance during the disease course of MASLD. Additionally, RASD1 regulated the lipid metabolism in liver by way of the PI3K/AKT/mTOR signaling. Therefore, targeting RASD1 is a promising druggable strategy for managing MASLD.

However, several limitations of this study must be mentioned. First, we only measured genes and proteins involved in DNL but not DNL itself, and whether RASD1 truly regulates DNL will require direct detection of DNL itself in future experiments. Second, the metabolomic analysis in this study focused on the lipidomics of cell samples; however, for a more precise and comprehensive effects of RASD1 on MASLD, a thorough metabolomic analysis using liver samples should be conducted in future studies. Third, albeit as a GTPase, RASD1 can be found with considerable expression not only in the cytoplasm but also within the nucleus of hepatocytes. Therefore, further investigations are needed to elucidate whether RASD1 regulates lipid metabolism through transcriptional or posttranscriptional mechanisms.

Conclusion

This study shows for the first a novel lipogenic role of RASD1 in MASLD via PI3K/AKT/mTOR signaling pathway (Fig. 8). RASD1 can be used as a promising biomarker for the prediction of MASLD progress and, also as a druggable target for treating the disease.

Supplementary Information

The online version contains supplementary material available at https://doi.org/10.1186/s12944-024-02419-z.

Supplementary Material 1

Supplementary Material 2

Supplementary Material 3

Acknowledgements

None is applicable.

Author contributions

GFZ, PPL, BJZ, and JL designed the study. GFZ, XLL, and ZYZ performed in vitro and in vivo experiments. JLZ, WFZ, EL, ZRB, SLC and CNC collected human samples and clinical data. GFZ, XLL, and ZYZ collected and analyzed all data, and prepared figures. GFZ wrote and edited the manuscript. PPL, BJZ, and JL revised the manuscript critically. All authors read and approved the final manuscript.

Funding

This work was supported by the National Natural Science Foundation of China (grant numbers 81971773 and 82272105), the Basic and Applied Basic Research Foundation of Guangdong Province (grant numbers 2023A1515011521, 2023A1515010475, 2022A1515011244, and 2020A1515010203), and the Medical Scientific Research Foundation of Guangdong Province (A2017421, 2016116212141586).

Data availability

No datasets were generated or analysed during the current study.

Declarations

Ethics approval and consent to participate

The Ethics Committee of the Fifth Affiliated Hospital of Sun Yat-sen University approved this study (approval number: [2020] L173-1). Informed consent was obtained from all patients before surgery. All animal experiments and related protocols were reviewed and approved by the Animal Ethics Committee of the Fifth Affiliated Hospital of Sun Yat-sen University (NO. 00287).

Consent for publication

Not applicable.

Competing interests

The authors declare no competing interests.

Received: 29 October 2024 / Accepted: 22 December 2024
Published online: 27 December 2024

References

1. Rinella ME, Lazarus JV, Ratziu V, Ratziu V, Francque SM, Sanyal AJ, et al. A multisociety Delphi consensus statement on new fatty liver disease nomenclature. J Hepatol. 2023;79:1542–56.
2. Eslam M, Newsome PN, Sarin SK, Anstee QM, Targher G, Romero-Gomez M, et al. A new definition for metabolic associated fatty liver disease: an international expert consensus statement. J Hepatol. 2020;73:202–9.
3. Miao L, Targher G, Byrne CD, Cao YY, Zheng MH. Current status and future trends of the global burden of MASLD. Trends Endocrinol Metab. 2024;29:S1043. -2760(24)00036 – 5.
4. Calzadilla BL, Adams LA. The natural course of non-alcoholic fatty liver disease. Int J Mol Sci. 2016;17:774.
5. Badmus OO, Hillhouse SA, Anderson CD, Hinds TD, Stec DE. Molecular mechanisms of metabolic associated fatty liver disease (MAFLD): functional analysis of lipid metabolism pathways. Clin Sci (Lond). 2022;136:1347–66.
6. Powell EE, Wong VW-S, Rinella M. Non-alcoholic fatty liver disease. Lancet. 2021;397:2212–24.
7. Lambert JE, Ramos-Roman MA, Browning JD, Parks EJ. Increased de novo lipogenesis is a distinct characteristic of individuals with nonalcoholic fatty liver disease. Gastroenterology. 2014;146:726–35.
8. ter Horst KW, Serlie MJ. Fructose consumption, lipogenesis, and non-alcoholic fatty liver disease. Nutrients. 2017;9:981.
9. Softic S, Cohen DE, Kahn CR. Role of dietary fructose and hepatic de novo lipogenesis in fatty liver disease. Dig Dis Sci. 2016;61:1282–93.
10. Shimano H, Yahagi N, Amemiya-Kudo M, Hasty AH, Osuga J, Tamura Y, et al. Sterol regulatory element-binding protein-1 as a key transcription factor for nutritional induction of lipogenic enzyme genes. J Biol Chem. 1999;274:35832–39.
11. Shimano H, Sato R. SREBP-regulated lipid metabolism: convergent physiology-divergent pathophysiology. Nat Rev Endocrinol. 2017;13:710–30.
12. Gosis BS, Wada S, Thorsheim C, Li K, Jung S, Rhoades JH, et al. Inhibition of nonalcoholic fatty liver disease in mice by selective inhibition of mTORC1. Science. 2022;376:eabf8271.
13. Kemppainen RJ, Behrend EN. Dexamethasone rapidly induces a novel ras superfamily member-related gene in AtT-20 cells. J Biol Chem. 1998;273:3129–31.
14. Tu Y, Wu C. Cloning, expression and characterization of a novel human ras-related protein that is regulated by glucocorticoid hormone. Biochim Biophys Acta. 1999;1489:452–6.

15. Cheng HY, Obrietan K. Dexras1: shaping the responsiveness of the circadian clock. Semin Cell Dev Biol. 2006;17:345–51.
16. Bass J, Takahashi JS. Circadian integration of metabolism and energetics. Science. 2010;330:1349–54.
17. Karatsoreos IN, Bhagat S, Bloss EB, Morrison JH, McEwen BS. Disruption of circadian clocks has ramifications for metabolism, brain, and behavior. Proc Natl Acad Sci U S A. 2011;108:1657–62.
18. Eckel-Mahan KL, Patel VR, Mohney RP, Vignola KS, Baldi P, Sassone-Corsi P. Coordination of the transcriptome and metabolome by the circadian clock. Proc Natl Acad Sci U S A. 2012;109:5541–6.
19. Lellis-Santos C, Sakamoto LH, Bromati CR, Nogueira TC, Leite AR, Yamanaka TS, et al. The regulation of Rasd1 expression by glucocorticoids and Prolactin Controls Peripartum maternal insulin secretion. Endocrinology. 2012;153:3668–78.
20. Jiang B, Lv Q, Wan W, Le L, Xu L, Hu K, et al. Transcriptome analysis reveals the mechanism of the effect of flower tea Coreopsis tinctoria on hepatic insulin resistance. Food Funct. 2018;9:5607–20.
21. Høyer KL, Høgild ML, List EO, Lee KV, Kissinger E, Sharma R, et al. The acute effects of growth hormone in adipose tissue is associated with suppression of antilipolytic signals. Physiol Rep. 2020;8:e14373.
22. Smith GI, Shankaran M, Yoshino M, Schweitzer GG, Chondronikola M, Beals JW, et al. Insulin resistance drives hepatic de novo lipogenesis in nonalcoholic fatty liver disease. J Clin Invest. 2020;130:1453–60.
23. Lomonaco R, Ortiz-Lopez C, Orsak B, Hardies J, Darland C, Finch J, et al. Effect of adipose tissue insulin resistance on metabolic parameters and liver histologyin obese patients with nonalcoholic fatty liver disease. Hepatology. 2012;55:1389–97.
24. Savage DB, Petersen KF, Shulman GI. Disordered lipid metabolism and the pathogenesis of insulin resistance. Physiol Rev. 2007;87:507–20.
25. Cha JY, Kim HJ, Yu JH, Xu J, Kim D, Paul BD, et al. Dexras1 mediates glucocorticoid-associated adipogenesis and diet-induced obesity. Proc Natl Acad Sci U S A. 2013;110:20575–80.
26. Song QQ, Rao Y, Tang GH, Sun ZH, Zhang JH, Huang ZS, et al. Tigliane Diterpenoids as a New type of Antiadipogenic agents Inhibit GRα-Dexras1 Axis in Adipocytes. J Med Chem. 2019;62:2060–75.
27. Seok JW, Kim D, Yoon BK, Lee Y, Kim HJ, Kim HJ, et al. Dexras1 plays a pivotal role in maintaining the equilibrium between adipogenesis and osteogenesis. Metabolism. 2020;108:154250.
28. Tong J, Cong L, Jia Y, He BL, Guo Y, He J, et al. Follistatin Alleviates Hepatic Steatosis in NAFLD via the mTOR dependent pathway. Diabetes Metab Syndr Obes. 2022;15:3285–301.
29. Chen J, Chen J, Huang J, Li Z, Gong Y, Zou B, et al. HIF-2α upregulation mediated by hypoxia promotes NAFLD-HCC progression by activating lipid synthesis via the PI3K-AKT-mTOR pathway. Aging. 2019;11:10839–60.
30. Wu H, Zhang X, Jia B, Cao Y, Yan K, Li JY, et al. Exosomes derived from human umbilical cord mesenchymal stem cells alleviate acetaminophen-induced acute liver failure through activating ERK and IGF-1R/PI3K/AKT signaling pathway. J Pharmacol Sci. 2021;147:143–55.
31. Dou C, Sun L, Wang L, Cheng J, Wu W, Zhang C, et al. Bromodomain-containing protein 9 promotes the growth and metastasis of human hepatocellular carcinoma by activating the TUFT1/AKT pathway. Cell Death Dis. 2020;11:730.
32. Lee S, Choi EJ, Cho EJ, Lee YB, Lee JH, Yu SJ, et al. Inhibition of PI3K/Akt signaling suppresses epithelial-to-mesenchymal transition in hepatocellular carcinoma through the Snail/GSK-3/beta-catenin pathway. Clin Mol Hepatol. 2020;26:529–39.
33. Grabinski N, Ewald F, Hofmann BT, Staufer K, Schumacher U, Nashan B, et al. Combined targeting of AKT and mTOR synergistically inhibits proliferation of hepatocellular carcinoma cells. Mol Cancer. 2012;11:85.
34. Wang SS, Chen YH, Chen N, Wang LJ, Chen DX, Weng HL, et al. Hydrogen sulfide promotes autophagy of hepatocellular carcinoma cells through the PI3K/Akt/mTOR signaling pathway. Cell Death Dis. 2017;8:e2688.
35. Vilà L, Elias E, Roca C, Ribera A, Ferré T, Casellas A, et al. AAV8-mediated Sirt1 gene transfer to the liver prevents high carbohydrate diet-induced nonalcoholic fatty liver disease. Mol Ther Methods Clin Dev. 2014;1:14039.
36. Virtue S, Vidal-Puig A. GTTs and ITTs in mice: simple tests, complex answers. Nat Metab. 2021;3:883–6.
37. Younossi Z, Anstee QM, Marietti M, Hardy T, Henry T, Eslam M, et al. Global burden of NAFLD and NASH: trends, predictions, risk factors and prevention. Nat Rev Gastroenterol Hepatol. 2018;15:11–20.
38. Rodriguez-Viciana P, Warne PH, Dhand R, Vanhaesebroeck B, Gout I, Fry MJ, et al. Phosphatidylinositol-3-OH kinase as a direct target of Ras. Nature. 1994;370:527–32.
39. Abdel-Wahab BA, Alqhtani H, Walbi IA, Albarqi HA, Aljadaan AM, Khateeb MM, et al. Piclamilast mitigates 1,2-dimethylhydrazine induced colon cancer in rats through modulation of Ras/PI3K/Akt/mTOR and NF-κβ signaling. Chem Biol Interact. 2021;350:109686.
40. Kumar S, Agnihotri N. Piperlongumine, a piper alkaloid targets Ras/PI3K/Akt/mTOR signaling axis to inhibit tumor cell growth and proliferation in DMH/DSS induced experimental colon cancer. Biomed Pharmacother. 2019;109:1462–77.
41. Chu H, Du C, Yang Y, Feng X, Zhu L, Chen J et al. MC-LR aggravates liver lipid metabolism disorders in obese mice Fed a High-Fat Diet via PI3K/AKT/mTOR/SREBP1 signaling pathway. Toxins (Basel). 2022;14(12).
42. Ye Q, Liu Y, Zhang G, Deng H, Wang X, Tuo L, et al. Deficiency of gluconeogenic enzyme PCK1 promotes metabolic-associated fatty liver disease through PI3K/AKT/PDGF axis activation in male mice. Nat Commun. 2023;14:1402.
43. Huang SJ, Chen SQ, Lin Y, Yang HY, Ran J, Yan FF, et al. Maternal nicotine exposure aggravates metabolic associated fatty liver disease via PI3K/Akt signaling in adult offspring mice. Liver Int. 2021;41:1867–78.
44. Sun C, Zhang J, Hou J, Hui M, Qi H, Lei T, et al. Induction of autophagy via the PI3K/Akt/mTOR signaling pathway by Pueraria flavonoids improves non-alcoholic fatty liver disease in obese mice. Biomed Pharmacother. 2023;157:114005.
45. He Y, Wang H, Lin S, Chen T, Chang D, Sun Y, et al. Advanced effect of curcumin and resveratrol on mitigating hepatic steatosis in metabolic associated fatty liver disease via the PI3K/AKT/mTOR and HIF-1/VEGF cascade. Biomed Pharmacother. 2023;165:115279.
46. Zhang CY, Tan XH, Yang HH, Jin L, Hong JR, Zhou Y et al. COX-2/sEH dual inhibitor alleviates hepatocyte senescence in NAFLD mice by restoring autophagy through Sirt1/PI3K/AKT/mTOR. Int J Mol Sci. 2022;23(15).
47. Wu YC, Yan Q, Yue SQ, Pan LX, Yang DS, Tao LS, et al. NUP85 alleviates lipid metabolism and inflammation by regulating PI3K/AKT signaling pathway in nonalcoholic fatty liver disease. Int J Biol Sci. 2024;20:2219–35.
48. Li J, Zhu L, Zhang YM, Chen H, Miao YF, Kang HX, et al. Sheng-Jiang Powder ameliorates high Fat Diet Induced nonalcoholic fatty liver Disease via inhibiting activation of Akt/mTOR/S6 pathway in rats. Evid-Based Compl Alt. 2018;2018:6190254.
49. Miao Y, Du Q, Zhang HG, Yuan Y, Zuo Y, Zheng H. Cycloheximide (CHX) Chase Assay to examine protein half-life. Bio Protoc. 2023;13:e4690.
50. Palaschak B, Herzog RW, Markusic DM. AAV-Mediated gene delivery to the liver: overview of Current technologies and methods. Methods Mol Biol. 2019;1950:333–60.
51. Srivastava A. AAV vectors: are they safe? Hum Gene Ther. 2020;31:697–99.
52. Porstmann T, Santos CR, Griffiths B, Cully M, Wu M, Leevers S, et al. SREBP activity is regulated by mTORC1 and contributes to akt-dependent cell growth. Cell Metab. 2008;8(3):224–36.
53. Duvel K, Yecies JL, Menon S, Raman P, Lipovsky AI, Souza AL, et al. Activation of a metabolic gene regulatory network downstream of mTOR complex 1. Mol Cell. 2010;39:171–83.
54. Peterson TR, Sengupta SS, Harris TE, Carmack AE, Kang SA, Balderas E, et al. mTOR complex 1 regulates lipin 1 localization to control the SREBP pathway. Cell. 2011;146:408–20.
55. Cornu M, Albert V, Hall MN. mTOR in aging, metabolism, and cancer. Curr Opin Genet Dev. 2013;23:53–62.
56. Wang H, Liu Y, Wang D, Xu Y, Dong R, Yang Y, et al. The Upstream pathway of mTOR-Mediated autophagy in Liver diseases. Cells. 2019;8:1597.
57. Hoxhaj G, Manning BD. The PI3K-AKT network at the interface of oncogenic signalling and cancer metabolism. Nat Rev Cancer. 2020;20:74–88.
58. Nam HH, Jun DW, Jang K, Saeed WK, Lee JS, Kang HT. Granulocyte colony stimulating factor treatment in non-alcoholic fatty liver disease: beyond marrow cell mobilization. Oncotarget. 2017;8:97965–76.
59. Lee SM, Dorotea D, Jung I, Nakabayashi T, Miyata T, Ha H. TM5441, a plasminogen activator inhibitor-1 inhibitor, protects against high fat diet-induced non-alcoholic fatty liver disease. Oncotarget. 2017;8:89746–60.

Publisher's note